Improving sensitivity to hydroxyl protons and simultaneous measurement of amide and NOE signals at 3T using variable pre-saturation power CEST (vCEST)

Daniel James Clark[1,2], Alex K Smith[3,4], Michael V Knopp[1], and Seth A Smith[3,4]

[1]*Wright Center of Innovation, Department of Radiology, The Ohio State University, Columbus, OH, United States,* [2]*Department of Biomedical Engineering, The Ohio State University, Columbus, OH, United States,* [3]*VUIIS, Department of Radiology and Radiological Sciences, Vanderbilt University, Nashville, TN, United States,* [4]*Department of Biomedical Engineering, Vanderbilt University, Nashville, TN, United States*

Purpose: Despite the wealth of studies suggesting the utility of CEST imaging, there is yet no clear advantage for the technique in clinical imaging at 1.5 and 3T. This is because (i) at clinical field strengths spectral separation (in Hz) is often less than the proton exchange rate, which causes the solute and water peaks to merge; (ii) even though sensitivity to exchange increases with irradiation power, so does direct water saturation, which will dominate the solute signal; (iii) the wide-band MT effect in tissue, normally invisible in MR imaging due to short T2 (~10 μs) will contribute to the measured CEST signal across the whole range of endogenous solutes unequally and asymmetrically; (iv) analysis of CEST z-spectra relies on asymmetry of the spectrum about Δω = 0 that is does not reflect the true solute CEST contribution in the presence of up-field molecules observed through NOE and the slight asymmetries of the MT and spill-over effects. In this study we propose a novel, variable-power CEST (vCEST) pre-saturation scheme for clinical scanners that mitigates the irradiation spill-over contribution to the z-spectrum. Specifically, this scheme, utilizing a variable power RF pre-saturation as a function of frequency offset, allows an indirect measurement of the direct water saturation (DWS) while simultaneously obtaining a direct measurement of the z-spectrum. For aqueous solutions without bound water, the z-spectrum is subtracted from the DWS resulting in a proton transfer ratio (PTR) that is composed of only solute CEST or NOE signal depending on the chemicals in solution. This technique has greater sensitivity to solutes with small chemical shifts and fast exchange rates, such as hydroxyls, than conventional CEST.

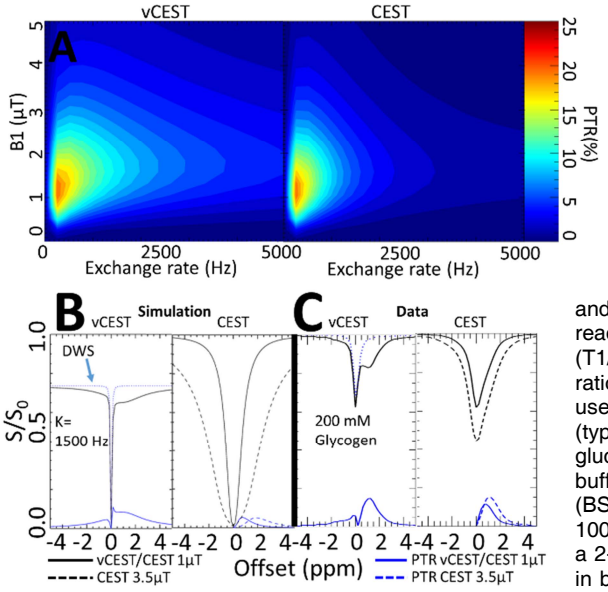

Methods: Theory. For any off-resonance pulse, there is some component of the effective B_1-field in the transverse plane that depends on the pulse amplitude and frequency offset. It can be shown that if the pre-pulse amplitude is varied as a function of frequency offset, $\omega_1(\Delta\omega) = \Delta\omega \tan\theta$, such that θ, the effective B_1-field angle, is constant then the DWS as a function of frequency offset is also constant: $DWS = \tan^2\theta / \left(\tan^2\theta + \frac{R_{1w}}{R_{2w}}\right)$. This relationship holds true as long as $\Delta\omega^2 \gg R_{1,water}R_{2,water}$. For most tissue, this product is on the order of 20 Hz, which corresponds to 0.04 ppm at 3T. Therefore, for almost all offsets of interest, the DWS should be constant. **Simuation.** Pulsed CEST experiments were simulated using the 2-pool Bloch-McConnell equations and the RF pulse integral method described in [**2**]. The model assumes a 100 ms pre-saturation pulse followed by an SPGR excitation and readout of a single k-space line. Therefore, at k-space center pre-saturation has reached a steady state. Pool properties are as follows: water (T1/T2=2400/90ms); hydroxyl (T1/T2=1000/29ms, pool ratio=0.01, chemical shift=1ppm); amine (T1/T2=1000/20ms, pool ratio=0.01, chemical shift=3ppm). A range of pulse amplitudes and exchange rates were used. **Phantoms.** Four 15ml falcon tubes were filled with solutions of PBS and glycogen (type IX bovine liver CAS 9005-79-2, Sigma-Aldrich) and four with solutions of PBS and glucose at concentrations of 20, 50, 100, 200 mM. Powdered NaOH was added for pH buffering to 7.4. Additionally, five tubes were filled with solutions of PBS and 10% albumin (BSA fraction V CAS 9048-46-8, Chem-Impex) with glycogen at concentrations of 0, 20, 50, 100, 200 mM. **Imaging.** Phantoms were imaged in a 3T Achieva (Philips, Cleveland) with a 2-channel transmit body coil and 8-channel receive head coil. Phantoms were mounted in bottles and submerged in a water-filled glass fishbowl. The following pulse sequences were used for parameter mapping: T1 map (IR-TSE, inversion times = 50, 100, 200, 400, 600, 900, 1200, 1800, 2500, 3000ms); T2 map (multi-echo TSE, T=40 – 20*40 ms), B0 map (WASSR, 3D SPGR with 50 ms/0.1 μT sinc-gauss pre-saturation pulse, 66 frequency offsets from -1 to +1ppm), B1 map (dual TR 25/100ms 3D SPGR), CEST (3D SPGR with 100ms/1μT and 3.5μT sinc-gauss pulse, 49 offsets from -5 to 5 ppm and one S0 image at -100kHz); vCEST(3D SPGR with 100 ms sinc-gauss pulse, RF amplitude varying by 1μT/1ppm with 0.25μT at 0ppm, 49 offsets from -5 to 5 ppm and one S0 image at -100kHz); vCEST reference (2 frequency offsets -10ppm and -100kHz, 10μT). **Image processing.** Both 1μT and 3.5μT CEST data were analyzed using WASSR B0 correction [**3**] and computing the asymmetry (PTR_{CEST}). The vCEST data was analyzed by computing the flattened DWS using measured T1, T2, B0 and B1 maps as inputs to a model as described above using only one pool. The DWS was computed out to ±10 ppm, and the difference between the computed z-spectrum and the vCEST reference scan at -10ppm was used to correctly place the DWS curve in relation to the measured z-spectrum. The measured z-spectrum was subtracted from the computed DWS creating a difference spectrum (PTR_{vCEST}). Voxel maps were made by measuring the AUC around the hydroxyl (0.75-1.75ppm) and amine (2.8-3.8ppm) shifts.

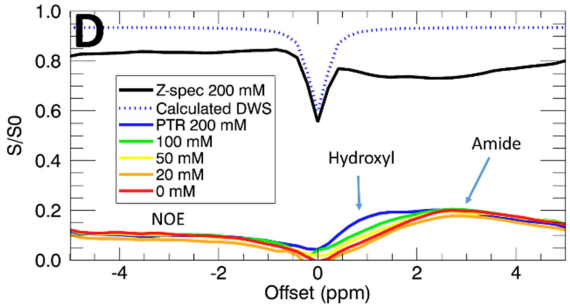

Results: Simulations show that pulsed vCEST should be more sensitive than conventional pulsed CEST for higher exchange rates (**figure A**). Simulation in **figure B** reveals that the hydroxyl signal should be a broad peak that extends past 0 ppm, which is confirmed by experiment in **figure C**. Additionally, the DWS contribution appears to be flat in the acquired z-spectra. For both glucose and glycogen phantoms, PTR_{vCEST} has a stronger linear correlation with concentration than PTR_{CEST} at both powers, as well as a wider range of values. In the BSA/glycogen phantoms, PTR_{vCEST} has a strong linear correlation with glycogen concentration. Additionally, the amide signal is observed at 3ppm as well as the NOE effect up-field from water (**figure D**).

Conclusion: The vCEST pulse sequence is more sensitive to hydroxyl moieties than standard CEST. Additionally, the PTR spectra both down- and up-field from water can be measured, thus doing away with the errors inherent in asymmetry calculations. This pulse sequence may allow detection of GAG molecules in cartilage imaging, as well as simultaneous measurements of amine and NOE signals in brain imaging, on clinical scanners.

References: 1. Portnoy S, Stanisz F. MRM. 2007 58:144-155. **2**. Kim M, van Zijl P, et al. 2009 MRM 61:1441-1450.